

# Laser Based Position Acquisition and Tracking in an Indoor Environment

Patric Jensfelt

Signal, Sensors & Systems  
Royal Institute of Technology  
SE-100 44 Stockholm

Henrik I. Christensen

Autonomous Systems  
Royal Institute of Technology  
SE-100 44 Stockholm

## Abstract

*In this paper we present a technique for acquisition and tracking of the pose of a mobile robot with a laser scanner. The position and orientation of the walls are the basis for estimating the pose of the robot. Validation gates filter out data that is believed to belong to the walls. For finding the parameters of the walls a two stage process with a local Range Weighted Hough Transform and a least squares method are implemented. Experimental results are shown to argue for the performance of the method.*

## 1 Introduction

Robots operating in a real world setting are subject to wheel slippage, drift in orientation etc. which implies that localization cannot only be based on odometric feedback. There is a need for feedback in terms of sensing of structures in the environment. The purpose of the feedback is twofold: i) localization and ii) detection of unexpected objects like obstacles. The sensing of structures in the environment can be done in a number of different ways as for example described in [2].

The most frequently used sensor for environmental mapping is the sonar sensor, due to its low price and ease of interpretation of the information. A major disadvantage of sonars is the slow sampling frequency and poor spatial resolution in its standard configuration. Good examples of use of sonars for mapping can be found in [9, 3, 6, 13]. For applications that require high spatial accuracy and/or higher temporal updating it is convenient to use a laser scanner as it offers higher resolution and improved sampling frequency.

In this paper an outline of how landmarks can be extracted from laser data and how such information

can be tracked over time to provide continuous localization information is presented.

In the first section we will describe the sensor that is used in the work. In Section 3 a short summary of previous work in this field will be given. Sections 4 and 5 describe in more detail absolute localization and position tracking respectively. In Section 6 results are presented and the last section concludes and discusses different paths for future research.

## 2 The Sensor system

Localization in a real world setting requires feedback regarding the position and orientation of structures in the environment. This can be achieved in a number of different ways using active (e.g. laser, sonar, IR, ...) or passive (e.g. vision sensors, gyros, wheel encoders) sensors. In this work we study the use of a laser scanner for localization.

### 2.1 The Laser Scanner

Compared to the widely used ultrasonic sonar sensor, the laser scanner is much more expensive and one has to weight price against performance when deciding for or against using the laser scanner. In many applications a laser scanner of this kind might be too expensive (e.g. powered wheel chairs and domestic vacuum cleaners), whereas other applications are less sensitive to the price (e.g. mining trucks). Laser range finders has been used by many researcher, both in the 2D scanning version [12, 5, 4, 10, 17] and in the range image version [1, 18, 15, 8, 16].

There are many advantages with laser scanners: high sampling rate, high angular resolution, fair range resolution, etc. Some of the drawbacks are: the information is restricted to a plane, the sensor is quite

expensive, some material appear as (almost) transparent for the laser (such as glass), etc.

## 2.2 Characteristics of the sensor

In our setup the laser sensor is a proximity laser scanner, the PLS 200 from SICK Electro-Optics. The SICK sensor can scan the environment at a rate of 25Hz. At this sampling frequency data are delivered at 333 kBaud on the serial port. Due to hardware limitations (max serial speed 38.4 kBaud) we use a sampling speed of 3Hz.

The SICK scanner uses a Time of Flight (TOF) ranging principle that is driven by a 6 GHz clock which provides a ranging resolution of 50 mm. The laser scanning is performed using a rotating mirror that rotates at 25Hz. In practice the sensor provides a polar range map of the form  $(\theta, r)$ , where  $\theta$  is the angle from  $0^\circ - 180^\circ$  discretized into  $0.5^\circ$  bins. Analyzing the output from the sensor it is apparent that the uncertainty of the data is uniformly distributed over the ranges  $[-25, 25]$  mm and  $[-0.25^\circ, 0.25^\circ]$ , respective. Converting the polar data into a Cartesian frame of reference we get:

$$\vec{c} = \begin{bmatrix} x \\ y \end{bmatrix} = r \begin{bmatrix} \cos \theta \\ \sin \theta \end{bmatrix}. \quad (1)$$

Let  $\Delta r$  and  $\Delta \theta$  define the size of the area over which the parameters  $r$  and  $\theta$  is distributed. The density functions can be written as  $f_r(r) = \frac{1}{2\Delta r}$  for  $r \in [\bar{r} - \Delta r, \bar{r} + \Delta r]$  and  $f_\theta(\theta) = \frac{1}{2\Delta \theta}$  for  $\theta \in [\bar{\theta} - \Delta \theta, \bar{\theta} + \Delta \theta]$ . The variance in the x and y direction can be derived with straight forward calculation assuming that  $r$  and  $\theta$  are independent. The result is:

$$\sigma_{xx} = \frac{1}{2}(\bar{r}^2 + \frac{1}{3}\Delta r^2) \left( 1 + \cos(2\bar{\theta}) \cos(\Delta \theta) \frac{\sin(\Delta \theta)}{\Delta \theta} \right) - \bar{r}^2 \cos^2(\bar{\theta}) \left( \frac{\sin(\Delta \theta)}{\Delta \theta} \right)^2 \quad (2)$$

$$\sigma_{yy} = \frac{1}{2}(\bar{r}^2 + \frac{1}{3}\Delta r^2) \left( 1 - \cos(2\bar{\theta}) \cos(\Delta \theta) \frac{\sin(\Delta \theta)}{\Delta \theta} \right) - \bar{r}^2 \sin^2(\bar{\theta}) \left( \frac{\sin(\Delta \theta)}{\Delta \theta} \right)^2 \quad (3)$$

$$\sigma_{xy} = \frac{1}{4}(\bar{r}^2 + \frac{1}{3}\Delta r^2) \cos(2\bar{\theta}) \cos(\bar{\theta}) \frac{\sin(\Delta \theta)}{\Delta \theta} - \bar{r}^2 \sin(\bar{\theta}) \cos(\bar{\theta}) \left( \frac{\sin(\Delta \theta)}{\Delta \theta} \right)^2 \quad (4)$$

This conversion of uncertainties was judged to be too messy and in the experiments the points were assumed to have an Gaussian distribution with a standard deviation of 50 mm both in x and y. This is a pessimistic approximation, but it has turned out to be adequate for our purposes.

## 3 Localization

As mentioned in Section 1, localization and navigation are the bases for solving many tasks. In this section there will be a brief overview of existing techniques and after that the method used in this paper will be described. The main emphasis will be put on the position tracking module. This module assumes that the position of the platform is known approximately. We will use a simple model of the environment where the room is modeled as a rectangle and the only available information is the length and width of the rectangle/room.

### 3.1 Previous Work

Localization has been studied extensively in the literature. Two main approaches are identified in [2], *landmark-based* and *map-based* localization. The landmark-based approach can be further split into three groups, depending on if the landmarks are *active artificial landmarks*, *passive artificial landmarks* or *natural landmarks*. An example of active artificial landmarks is the GPS system. Passive landmark systems are very widely used in industry, e.g., line markings on the floor and signs on the walls. The natural landmarks are those that have not been put there for the purpose of aiding the navigation task: walls, doors, corners, etc. Among the map-based techniques the occupancy-grid technique has been widely used since it was introduced by Moravec and Elfes [14]. The map-based technique tries to match a local map acquired through the use of some sensor(s).

Introducing odometric feedback in the above mentioned approaches will improve their performance, in some cases significantly. By using odometry, more or less accurate predictions of the movement of the platform can be used to reduce the area in which to look for landmarks or the possible movements when matching maps. Using odometry also provides a means for keeping track of the position when no sensor data is available. When using odometry it is important to realize that there are situations in which the odometry will give very bad results, e.g., when passing over thresholds or when driving in uneven terrain. In those situations the system must be robust enough to realize the failure of the odometry.

## 4 Absolute localization

Localization can be divided into two parts: i) initialization and ii) maintenance. The initialization is

responsible for providing an initial position estimate when the robot is turned on. Based on an approximate model of the environment and a data set, the translation and rotation (the pose) of the robot must be estimated. Once the system has been properly initialized, the maintenance part is responsible for online updating of the position estimate. In this work it will be assumed that the robot only operates in a single room, which can be approximated by a rectangle. The reason being that we want to use the simplest possible map of a room and then determine how well the system can be initialize and maintain a robust estimate of its pose.

We have chosen to use the *Angle Histogram* [11] to do absolute localization. The angle histogram will give two possible locations of the robot as the rectangular room is symmetric as described in the next section.

#### 4.1 The Angle Histogram

The angle histogram methods was introduced in [11]. The idea behind the angle histogram is simple. The main characteristic of a regular office environment room is that there are straight walls and that the walls are either parallel or perpendicular. The algorithm assumes that data is available from a full 360° scan of the room. Therefore two scan are taken and the data is transformed into the same coordinate system (a robot fixed coordinate system). Let  $\mathbf{x}_i$ ,  $i = 1 \dots N$  be the vector containing the measurements in Cartesian coordinates (see Figure 1). The angle histogram algorithm method we used can be described as follows:

1. The first step is to try and find the orientation of the walls, by studying the angle between consecutive data points. Using points next to each other turns out to give a very noisy response so it is better to look at the angle between points with  $L$  points in between them, in our case we use  $L = 20$ . Let us call the consecutive angles  $\alpha_i$ ,  $i = 1 \dots N - L$ .
2. A histogram over  $\alpha_i$  is then created over the range 0°-180°. In a normal room, there will be two distinct peaks in the histogram corresponding to the two main orientations of the walls. Note that by taking modulo 180°, parallel walls are mapped to the same angle. Figure 2 shows an example histogram. Assuming that the maximum peak corresponds to an angle  $\beta$ , this means that the orientation of the robot must be  $\beta + i * 90^\circ$ ,  $i = 0, \dots, 3$ .
3. The original data is then rotated by the angle  $\beta$

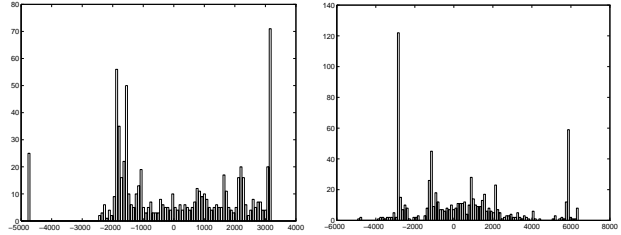


Figure 4: Histogram over the x-values and y-values in the rotated data set.

corresponding to the maximum peak. If the algorithm is successful, the walls should now be oriented parallel to the coordinate axis of the robot (see Figure 3).

4. By analyzing the histogram for the  $x$  and  $y$ -distribution (see Figure 4) in the rotated data the position of the robot can be narrowed down to two possible cases. A voting scheme is used to determine what histogram to match with which pair of walls. The two hypotheses are *i*) histogram 1 belongs to wall pair 1 and *ii*) histogram 2 belongs to wall pair 1. Each peak in the histogram vote for a certain position relative to a wall. The more peaks that agree on the same position the higher the vote. Each peak vote with the strength of that peak, i.e. strong wall responses carry much weight. In order to decide whether the robot is at position  $(x, y)$  or  $(x_{size} - x, y_{size} - y)$ <sup>1</sup> more information has to be used. One way to solve it is to assume that the approximate orientation (with an error less than 90°) of the robot is known a-priori (for example from a compass). Another solution would be to try to use information about the location of other structures in the environment such as doors. In our case we assume the existence of a compass that can give us information that can be trusted enough to pick one of two hypotheses that differ in orientation by 180°.

## 5 Position Tracking

### 5.1 Idea

Doing an absolute localization is a computationally costly process. But even more important is maybe the fact that it also requires control of the movement of the platform or, to be exact, the movement of the sensor. Therefore the idea is to do the absolute localization

<sup>1</sup> $x_{size}$  and  $y_{size}$  is the size of the room

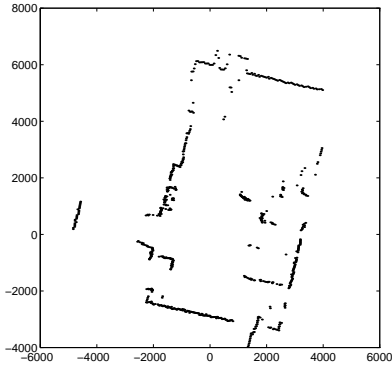


Figure 1: The original SICK data.

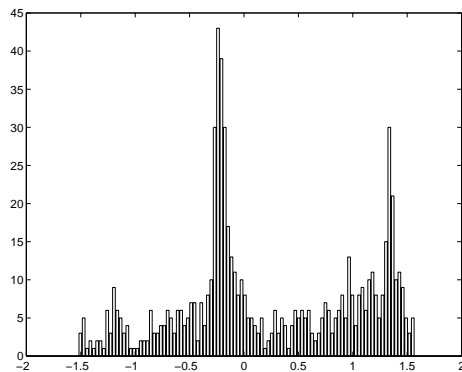


Figure 2: Angle histogram.

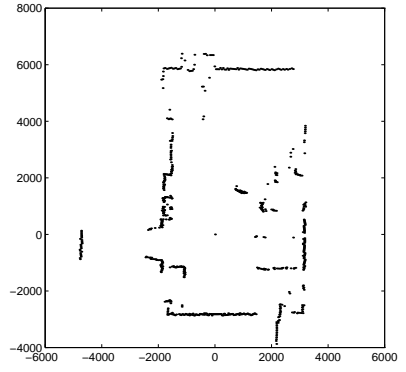


Figure 3: The data after the rotation.

tion only once and after that track the position of the robot using odometry and laser data. Since we use a map that only consists of two numbers, the length and width of the room, we only have information about the location of the walls. Therefore only the walls can be tracked. It is however relatively easy to extend the method to track  $n$  structures in the environment.

In this paper we will present a Kalman filter based technique. An important property of the Kalman filter is the lack of ability to revise the use of measurements in the past, that later turn out to have been erroneously associated with a certain feature<sup>2</sup>. Therefore it is of importance that the risk of making a mistake, when associating data with a feature, be as small as possible. With the use of the odometry the location of the robot can, in most cases, be predicted with a high accuracy, and by using validation gates for the data, the risk is kept small, but not negligible.

The pose of the robot will be represented by  $\mathbf{x}_k = (\mathbf{x}, \mathbf{y}, \theta)^T$ . The system can be described by

$$\mathbf{x}_{k+1|k} = \mathbf{x}_{k|k} + \mathbf{g}_k + \mathbf{w}_k \quad (5)$$

where  $\mathbf{g}_k$  is the input from the odometry and  $\mathbf{w}_k$  represents the process noise. The measurement equation can be described by

$$\mathbf{z}_{k,i} = \mathbf{h}_i(\mathbf{x}_k) + \mathbf{v}_{k,i}, \quad i = 1, \dots, N \quad (6)$$

where  $\mathbf{h}_i$  represents a possibly nonlinear measurement function and  $\mathbf{v}_{k,i}$  is the corresponding measurement noise.

## 5.2 The Filtering of Data

The filtering of data is performed as follows (see dashed rectangle in Figure 5).

<sup>2</sup>This can of course in principle be solve by saving all the data from the past.

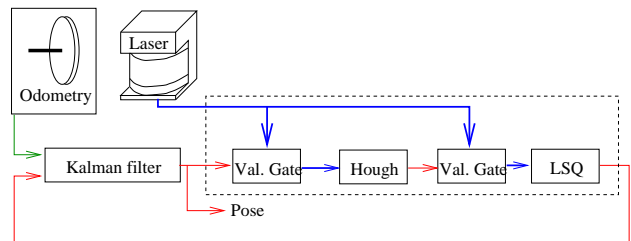


Figure 5: Signal flow in the localization module.

1. Data is run through four validation gates, one for each wall. This could be extended to be  $n$  walls instead as well as other features.
2. Perform a local Range Weighted Hough Transform<sup>3</sup> [10] on the validated data, only allowing parameters close to the predicted.
3. Run the raw data through another validation gate with parameters adjusted according to the result of the local RWHT.
4. Do a Least Squares fit.

This will give us between 0 and 4 walls. Each wall will have an uncertainty attached, which depends on the data that was used to hypothesize the location of the wall. We have used the implementation from [7] for the least square algorithm which also provides estimates of the uncertainty in the line parameters. The representation of the walls is  $(\rho, \varphi)$  where  $\rho \in [0, \infty)$  and  $\varphi \in [0, 360^\circ)$ .

<sup>3</sup>Like a standard Hough transform except that the vote of a point far away carries more weight than a point close to the sensor. The idea is that points close to the sensor tend to be closer together and therefore they will influence more unless a range weight is introduced.

### 5.2.1 The Validation Gates

Given an initial estimate of the pose of the robot, it is possible to predict where the wall(s) will be in the data. The uncertainty in the pose as well as the quality of the data will determine the size of the validation gates. The locations of the validation gates is based on the prediction of the pose of the robot and the map of the current room.

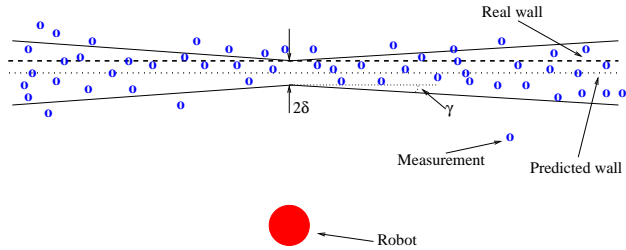


Figure 6: Each validation gate is defined by two parameters, the size of the waist,  $\delta$  and the opening angle,  $\gamma$ . Note that the error in the prediction of the wall and the size of the validation gate were scaled for illustration purposes.

Experience indicate that the opening angle  $\gamma$  should be set to zero or at least be kept very small independent of the uncertainty in orientation. This is motivated by the use of the *Range Weighted Hough Transform* (RWHT) [10] which will be effected more by outliers the further away they are.

### 5.3 Pose Tracking

In each cycle of the tracking loop the information from the odometry and the laser scanner is fused into an estimate of the pose of the robot. Odometry data is available at a higher sampling rate than the laser data and can be used alone to update the pose of the robot in between laser scans. As the robot in our experiments has been moving on a largely planar floor with a high coefficient of friction, the process noise ( $\mathbf{w}_k$  in (5)) is small compared to the measurement noise. This means that we will have a filter that will have a very hard time handling errors in the odometry readings. Typical situations in which this might occur are when the robot: i) touches a wall and the platform is rotated, ii) drives over some obstacle (cable, threshold, etc.).

In order to handle this problem it is necessary to introduce some kind of condition on the success of the matching process. If no walls are matched for some time, it is a strong indication that the estimate of the position might be wrong. In such a case the estimate must be re-initialized by doing a new absolute localization (the last pose estimate could potentially be used

	$x$	$\Delta x$	$y$	$\Delta y$	$\theta$	$\Delta \theta$
Pos1	3420	-30	7650	60	119	-0.2
Pos2	2470	120	6440	-30	119	-2
Pos3	1380	10	7870	-7070	118	+0.8
Pos3b	1380	10	7870	-50	118	+0.8
Pos4	3940	-50	3900	10	116	-0.8
Pos4b	3940	-50	3900	10	116	-0.8

Table 1: Results of the absolute localization. Four different locations have been tested and in two of the locations two different environmental settings were tested. The only time the routine failed (Pos3) was when it was placed close to one of the short wall and had three chairs lined up in front of it. In this case the algorithm could not distinguish the back of the chairs from a wall.  $\Delta x$ ,  $\Delta y$  and  $\Delta \theta$  represent the errors in the three different components.

as a starting point for this). Alternatively one could increase the size of the validation gates, corresponding to an increased uncertainty in the state estimate, so one might also add a deterministic amount of noise to  $P$  in case of bad matching data. Care has to been taken to make sure that the gates do not become too big since the chance for erroneous matches increase with the size of the gates. This has not been implemented yet.

The pose is updated with the information from each wall sequentially, using (6). It is assumed that the covariance between the parameters of the walls are uncorrelated, to simplify computations.

## 6 Experimental Results

In this section the result of several experiments, designed to verify the performance of the system, will be presented. The presentation will be divided into two parts: one for absolute localization and one for pose tracking. The experiments were carried out in our robot lab that has been furnished like a living room in order to insure that relevant questions are being answered, i.e. the system has to be able to operate in a normal house environment. Figures 7 and 8 show the living room from two different view points.

### 6.1 Absolute Localization

In this test the robot was placed at different locations in a room and the algorithm was run to estimate the pose of the robot. To be able to evaluate the result



Figure 7: View 1 of the living room.



Figure 8: View 2 of the living room.

of these experiments it is necessary to know the resolution of the histograms used to estimate orientation and position of the robot. When estimating the angle of the robot, the histogram had a resolution of  $1.8^\circ$  and the histogram giving the position had a resolution of 200 mm. At each point five experiments were performed. As the resolution of the histograms were low, the position that was estimated by the absolute localization algorithm was more or less the same in all five experiments at all locations. More or less in this case means that when the robot was placed close to the middle of two histogram cells, the estimated position shifted between those two positions.

## 6.2 Position Tracking

To verify the performance in the case of position tracking, the true position at each time instant should ideally be known. This is in practice not possible.

The questions we want to answer with the experiments are: I) is the method robust over time, II) how does it compare with the odometry, III) repeatability, IV) how accurate is it and V) how important is the choice of walls to “look” at. The following two experiments were done:

### 6.2.1 Experiment 1

In this experiment the robot was given a chain of goal points to which it had to go. The robot is not forced to come exactly to every goal point, only within 100 mm of it. At the end position though, the requirements are harder and the robot is told to stop within 5mm of the start/end point. As the test was constructed to test the robustness over time as well as to make

a comparison with the odometry, the test took about 15-20 minutes to perform. By calculating the distance between the goal points in the chain and multiplying by the number of laps around the chain, the theoretical distance the robot had to travel was found to be 180 m.

The robot was driven totally autonomous and an avoid behavior was active during execution to make sure that the robot did not run into any obstacles. We let the start and the end position be the same to make the calculations easier. The outline of the experiment is:

1. Place the robot at the desired start/end position.
2. Zero the robot, i.e. reset the odometry.
3. Measure the pose of the robot
4. Do absolute localization
5. Let the tracking unit run until the uncertainty in the position has decreased under a certain threshold (in this case both  $\sigma_x$  and  $\sigma_y$  has to be less than 25 mm). This is to give the system a good estimate of the starting position to which it is supposed to go back.
6. Let the robot make the trip around the chain of goal points back to the start/end point, run for approximately 18 minutes.
7. Read the result of the odometry.
8. Measure the pose of the robot.

As the robot moved around in the room for almost 20 minutes when completing the chain of goal points

	Run 1		Run 2	
	start	stop	start	stop
$x$	2976	2960	3054	3053
$\Delta x$	15	42	14	6
$\Delta x_{od}$	-	723	-	1220
$y$	7276	7288	7300	7282
$\Delta y$	42	39	44	49
$\Delta y_{od}$	-	48	-	39
$\theta$	91.96	120.0	73.64	102.1
$\Delta \theta$	1.85	2.1	2.33	2.12
Time	1074 sec		1125 sec	
Dist	181 m		181 m	
Speed	0.17 m/s		0.16 m/s	

Table 2: Results of Experiment 1, designed to test robustness over time, repeatability and make a comparison with odometry.  $x$  denotes the true x-coordinate,  $\Delta x$  is the error in the tracking units estimate,  $\Delta x_{od}$  error in odometry based estimate, etc ... The total time for the tests is given along with the theoretical distance traveled and the average speed.

and was able to keep track of its position, robustness can be argued for. Even better performance would have been achieved by actively controlling the direction in which the sensor was looking. Table 2 shows that the repeatability was fairly good since the robot returned to almost the same position. The odometry was helpless when the platform drifted for about 30° during each test. This was due to a badly calibrated wheel system on our robot. A bias can be noted in the results. In the y direction the bias was almost the same in all in the four measurements that were made (about 40 mm), and in the x direction the bias was at least always positive. The source of this bias was believed to be an offset in the laser data and poor measurements of the position and orientation of the sensor in relation to the platform.

### 6.2.2 Experiment 2

In this experiment the robot was placed at an arbitrary position in the room. It did absolute localization, headed for a specific goal point and stopped when within a certain radius of the point (in this case 5 mm). To test the effects of the direction of attention, the sensor was facing different directions in the tests. During the execution of each test the sensor was facing in the same direction except when the robot did the absolute

localization. In our setting one of the long walls was covered with book shelves and the visible part of the more than 8 meter long wall was only about a meter.

The result of this experiment showed that the method provided means to position the robot at a given location with an accuracy of  $(\sigma_x, \sigma_y) = (19, 18)$ mm. A small bias was still present in the data (about 10 mm in both x and y), but most of it had been removed by refining the parameters. When it comes to the choice of walls to direct attention to, the question does not have a simple answer. As long as the sensor can pick up enough points from a wall to form an estimate of the position of the wall it does not matter much if the wall is occluded in parts by bookshelves, waste bins, etc, as long as long as the estimate of the position is good enough to make the validation gate so small that only data that comes from the actual wall is used. A more thorough investigation of the effects of the choice of direction of attention has to been done to answer the question in more detail.

Due to the fact that the odometry is very good over short distances, especially when there is compensation for the drift in orientation, it was found that it was not necessary for the sensor to see the wall at all times and still keep accurate track of the position and orientation of the robot.

## 7 Conclusion and the Future

This paper has presented a method for tracking the pose of a mobile robot using a laser scanner. In principle any scanning sensor with about the same angular resolution can be used in its place. It has been shown that the method provides good positioning accuracy and robustness. A more accurately calibrated system and more accurate ground truth measurements are required to establish exactly how good it is.

The reader should keep in mind that one of the driving issues of this research is to see how far one can come with a very simple model of the world. A model that in our case consist only of the length and width of rooms that are modeled as being rectangular. The performance will of course improve by introducing information from other features and structure, but the aim is to minimize the need for detailed information.

In the future the method will be extended to a situation with many rooms, and potentially also with rooms of different shapes than rectangular. To extend the position tracking technique to handle rooms of different shapes as long as they can be represented with line segments is straight forward. It will only change the measurement equation (the h-function) in (6).

There are still many open field for further investigations, e.g.:

- How much occlusion of the wall can the method handle?
- How to direct the attention of the sensor?
- How to discover and recover from larger error in odometric data?
- How would more advanced estimation methods perform?

## 8 Acknowledgment

The research has been carried out at the Centre for Autonomous Systems at the Royal Institute of Technology, and is sponsored by the Swedish Foundation for Strategic Research.

## References

- [1] C. Andersen, C. Madsen, J. Sorensen, N. Kirkeby, J. Jones, and H. Christensen. Navigation using range images on a mobile robot. *IEEE Transactions on Robotics and Automation*, 10(2-3):147–160, 1992.
- [2] J. Borenstein, H. Everett, and L. Feng. *Navigating Mobile Robots: System and Techniques*. A K Peters, Ltd., 1996.
- [3] J. Borenstein and Y. Koren. The vector field histogram - fast mobile obstacle avoidance for mobile robots. *IEEE Transactions on Robotics and Automation*, 7(3):278–288, June 1991.
- [4] S. Borthwick, M. Stevens, and H. Durrant-Whyte. Position estimation and tracking using optical range data. In *Proc. of International Conference on Intelligent Robots and Systems*, pages 2172–2177. IEEE/RSJ, 1993.
- [5] M. Buchberger, K. W. Jörg, and E. von Puttkamer. Laserradar and sonar based world modeling and motion control for fast obstacle avoidance of the autonomous mobile robot mobot-iv. In *Proc. of International Conference on Robotics and Automation*, volume 1, pages 534–40. IEEE, 1993.
- [6] J. Crowley. Dynamic world modeling for an intelligent mobile robot using a rotating ultra-sonic ranging device. In *Proc. of International Conference on Robotics and Automation*, volume 1, pages 128–135. IEEE, 1985.
- [7] R. Deriche, R. Vaillant, and O. Faugeras. *From Noisy Edges Points to 3D Reconstruction of a Scene : A Robust Approach and Its Uncertainty Analysis*, volume 2, pages 71–79. World Scientific, 1992. Series in Machine Perception and Artificial Intelligence.
- [8] G. Dudek, P. Freedman, and I. Rekleitis. Just-in-time sensing: efficiently combing sonar and laser range data for exploring unknown worlds. In *Proc. of International Conference on Robotics and Automation*, volume 1, pages 667–672. IEEE, 1996.
- [9] A. Elfes. Sonar-based real-world mapping and navigation. *IEEE Journal of Robotics and Automation*, RA-3(3):249–265, June 1987.
- [10] J. Forsberg, P. Åhman, and Å. Wernersson. The hough transform inside the feedback loop of a mobile robot. In *Proc. of International Conference on Robotics and Automation*, volume 1, pages 791–798. IEEE, 1993.
- [11] R. Hinkel and T. Knieriemen. Environment perception with a laser radar in a fast moving robot. In *Symposium on Robot Control*, pages 68.1–68.7, October 1988.
- [12] P. Hoppen, T. Knieriemen, and E. von Puttkamer. Laser-radar based mapping and navigation for an autonomous mobile robot. In *Proc. of International Conference on Robotics and Automation*, volume 2, pages 948–953. IEEE, 1990.
- [13] J. J. Leonard and H. F. Durrant-Whyte. *Directed Sonar Sensing for Mobile Robot Navigation*. Kluwer Academic Publisher, Boston, 1992.
- [14] H. Moravec and A. Elfes. High resolution maps form wide angle sonar. In *Proc. of International Conference on Robotics and Automation*, pages 116–121. IEEE, 1985.
- [15] F. Nashashibi, M. Devy, and P. Fillatreau. Indoor scene terrain modeling using multiple range images for autonomous mobile robots. In *Proc. of International Conference on Robotics and Automation*, volume 1, pages 40–46. IEEE, 1992.
- [16] J. Neira, J. Horn, D. Tardós, and G. Schmidt. Multi-sensor mobile robot localization. In *Proc. of International Conference on Robotics and Automation*, volume 1, pages 672–679. IEEE, 1996.
- [17] G. Weiss and E. von Puttkamer. A map based on laserscans without geometric interpretation. *Intelligent Autonomous Systems*, pages 403–407, 1995.
- [18] J. Yang and Y. Wu. Detection for mobile robot navigation based on multisensor fusion. In *Proc. of SPIE*, volume 2591, pages 182–192, 1996.